ELSEVIER

Journal of Power Sources 109 (2002) 105–110

JOURNAL OF POWER SOURCES

www.elsevier.com/locate/jpowsour

Application of electrochemically prepared carbon nanofibers in supercapacitors

P.V. Adhyapak[a], Trupti Maddanimath[b], Sushama Pethkar[b], A.J. Chandwadkar[b], Y.S. Negi[a], K. Vijayamohanan[b,*]

[a]*Centre for Materials for Electronics Technology, Panchwati, Off Pashan Road, Pune 411008, India*
[b]*National Chemical Laboratory, Dr. Homi Bhabha Road, Pune 411008, India*

Received 1 October 2001; accepted 16 January 2002

Abstract

Supercapacitive behavior of electrochemically synthesized carbon nanofibers by the controlled reduction of chloroform at room temperature is demonstrated. The important advantage of the electrochemical route is in situ functionalization of carbon fibers (CFs), which can be controlled by the nature of the precursor. The FTIR spectrum of as-prepared CFs reveals substantial amounts of functionalized species, namely, –OH, =O, –COOH, etc., while scanning electron micrographs show CFs packed in bundles of 25 μm. The presence of amorphous carbon as well as traces of a graphitic phase is confirmed by means of thermogravimetric analysis (TGA) and X-ray diffraction (XRD), respectively. The capacitive behavior of the carbon nanofibers is studied in terms of charge–discharge curves and cyclic voltammograms. A specific capacitance of 28 F g^{-1} is obtained for a measured surface area of 78 m^2 g^{-1}. Thermal treatment does not cause a change in surface structure as well as capacitive behavior of the carbonaceous materials although there is an increase in surface area to 592 m^2 g^{-1}. © 2002 Published by Elsevier Science B.V.

Keywords: Electrochemical synthesis; Carbon fibers; Functionalized carbon fibers; Supercapacitance; Charge–discharge

1. Introduction

Supercapacitors, also known as electrochemical capacitors, are being extensively studied due to an increasing demand for energy-storage systems. These devices offer many advantages over conventional secondary batteries, which include the ability of fast charge propagation, long cycle-life and better storage efficiency. This has made them popular as promising energy sources for electric vehicles, digital telecommunication systems, uninterruptible power supplies for computers, pulse lasers, etc. [1–3].

In the past few years, considerable interest has been focused on the application of carbonaceous materials as an electrode for supercapacitors because of their chemical inertness and easy processibility. In addition, carbon being amphoteric in nature exhibits good electrochemical properties from donor to acceptor state, which makes it an attractive material for supercapacitors. Recent developments in carbon nanotubes (CNTs) have demonstrated the excellent ability of these nanostructures for the accumulation of charges [4,5] because of their unique characteristics, viz. high surface area, high electrical conductivity, low density and excellent chemical stability [6–8]. Reports on electrochemical applications of CNTs, such as for the storage of hydrogen for fuel cells [9,10], lithium-ion secondary batteries [11,12], and supercapacitors [13–15] are available in the literature.

In the present paper, we demonstrate a supercapacitor based on partially crystalline, electrochemically synthesized, carbon fibers (CFs). For example, fibers of amorphous conductive polymers, such as polyaniline and polypyrrole are electrochemically synthesized in either porous template membranes or with electrode surface defects [16]. CFs, like CNTs, can be highly ordered as those derived from carbon arc [17,18] or highly disordered as the materials obtained from gas-phase pyrolysis [19,20]. Electrochemical synthesis of elemental carbon is, in principle, accomplished either by anodic oxidation (e.g. from hydrocarbons) or cathodic reduction (e.g. from carbon oxides or halides) [21]. Electrochemical synthesis provides good control over material composition as well as growth rate.

2. Experimental

All the chemicals used were obtained from Aldrich. The solvents were distilled before use. Electrochemical deposition

* Corresponding author. Tel.: +91-20-589-3300; fax: +91-20-589-3044.
E-mail address: viji@ems.ncl.res.in (K. Vijayamohanan).

0378-7753/02/$ – see front matter © 2002 Published by Elsevier Science B.V.
PII: S0378-7753(02)00049-6

was carried out in a two-compartment cell, with the graphite counter electrode separated from the working electrode by a glass frit. CFs were collected on a molybdenum electrode surface during cathodic decomposition of chloroform at room temperature using a similar procedure to that reported by Herrick II et al. [22]. The molybdenum electrode (5 cm × 2 cm) was chemically polished in a solution which was a mixture of perchloric acid, sulfuric acid and nitric acid in the volume ratio 1:1:1. The electrolytic deposition solution, typically, consisted of 60 ml of $CHCl_3$ with 3 g of tetrabutylammonium bromide dissolved in acetonitrile as a supporting electrolyte.

The deposition was carried out for 3 h with a current density of 9.5 mA cm^{-2}. The CF sample (hereafter termed 'as-prepared CFs') collected from the molybdenum electrode was washed thoroughly with acetonitrile and dried at 100 °C to remove loosely adsorbed impurities. This carbonaceous material was then thermally-treated at 300 °C in air.

Scanning electron microscopy (SEM) images were obtained by means of a Philips 30 XL instrument which was operated at 10 kV in the secondary electron imaging mode. Transmission electron imaging was performed on a JEOL 1200 EX microscope operated at 100 kV. The sample was prepared by dispersing the extracted fibers in methanol. The imaging was enabled by depositing a few drops of the suspension on a carbon-coated, 400 mesh, copper grid. The solvent was allowed to evaporate before imaging.

The infrared spectra of the composite in the transmission mode were recorded on a Perkin-Elmer Spectrum 2000 FTIR spectrophotometer. The sample pellet was prepared by mixing 1 mg of carbon material in 150 mg of KBr. The spectra were collected in the range 4400–450 cm^{-1}. X-ray diffractograms of CFs were recorded on a Philips PW 1710 diffractometer using Cu Kα ($\lambda = 1.541$ Å) radiation. The composition was further studied with a thermogravimetric analyzer (Mettler toledo 851). The experiment was carried out at a 10 °C min^{-1} ramp rate from 25 to 900 °C with an airflow rate of 80 ml min^{-1}.

The dc capacitance was evaluated from charge–discharge curves in 6 M KOH solution. The CFs 95 wt.% and poly-(vinyl styrene) (PVS) 5 wt.% as a binder were mixed in tetrahydrofuran (THF). The paste obtained was then applied on both sides of a thin nickel mesh (0.4 cm × 0.3 cm). After evaporation of the THF, the carbon electrode was formed by pressing the sample with steel moulder. The cell was charged to 0.95 V at a constant current of 0.6 mA and discharged at same current until the voltage decreased to 0 V. The dc capacitance was then estimated from the formula $C = I(\Delta t/\Delta v)$ where, I is the discharge current in amperes and Δt the time period in seconds required for the potential difference of Δv in volts.

Cyclic voltammograms were obtained by means of a scanning potentiostat model 362 and a recorder model REO 151 in 6 M KOH using a standard cell which used carbon (pressed on nickel mesh) as the working electrode, platinum as the counter electrode, and a saturated calomel electrode (SCE) as the reference electrode.

3. Results and discussion

Carbon nanofibers were synthesized by an electrochemical route from chloroform precursor. The composition of as-prepared CFs and the quantitative content of each species were estimated by thermogravimetric analysis (TGA). The TGA curve and the differential curve of the as-prepared CFs are shown in Fig. 1. From the thermogram, it is clear that the initial burning temperature is ~200 °C and the decomposition progresses in two steps. The weight loss at 200 °C corresponds to amorphous carbon along with some fraction of functionalized moieties, whereas, the subsequent weight loss at ~460 °C can be assigned to CFs and is in accordance with published studies [23]. The CFs show complete evaporation near 900 °C. The remaining fraction suggests embedded small crystalline domains of graphitic carbon. The presence of graphite-like carbon is further supported by

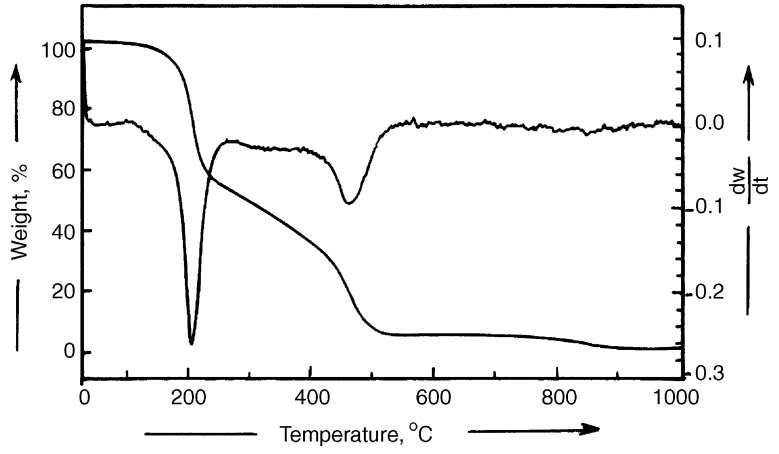

Fig. 1. TGA curve of as-prepared carbon nanofibers recorded at 10 °C min^{-1} ramp rate from 25 to 900 °C with an airflow rate of 80 ml min^{-1}, and the respective differential.

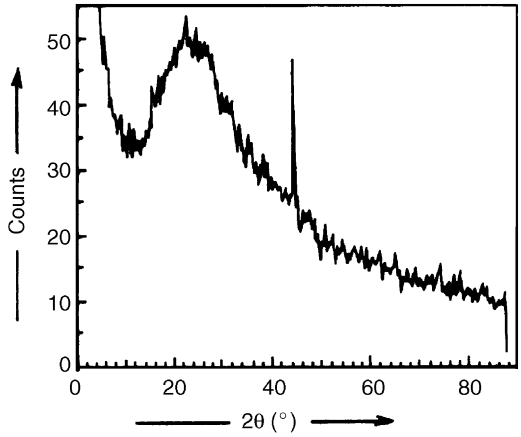

Fig. 2. XRD pattern of as-prepared carbon nanofibers showing small domains of turbostatic structure.

X-ray diffraction (XRD). The XRD pattern of CFs (Fig. 2) exhibits a strong peak located at $2\theta = 44.4^\circ$, consistent with the (10) index of graphite. The broad peak $\sim 25^\circ$ can be assigned to the (2 0 0) line of graphite. The broadening of this peak indicates the existence of graphite plane segments in small domains and the structure appears to be turbostatic in nature [24]. The content of each species in the CFs is quantitatively estimated from the DTA curve. The calculated yields of amorphous carbon and CFs are 42.3 and 24.8%, respectively.

A typical scanning electron micrograph of CFs (Fig. 3(a)) displays bundles of fibers entangled with each other and a significant content of white matter, which consists mainly of amorphous carbon. The fibers are closely packed in a bundle of approximately 25 μm in width with amorphous carbon appearing as a filter material. This morphology suggests higher deposition rates. It is also noted that the threshold current density required for the reduction of substituted carbon tetrachlorides is significantly higher than that required for the unsubstituted counterpart, which is the prime factor in deciding the structure of the deposited CFs. In addition, because of incomplete reduction of chloroform at the electrode, an amorphous phase of carbon remains chemically bound to the fibers. The amorphous carbon can be selectively removed by thermal annealing. Selective etching is generally expected due to the faster oxidation rates of amorphous carbon [25]. As the initial burning of CFs was to be 200 °C from the TGA curves, the as-prepared material was subjected to thermal annealing at 300 °C to ensure efficient etching of amorphous content. After annealing for 6 h in air, a weight loss of nearly 54% of the original sample was observed, which is substantially more than that estimated from a DTA plot, viz. 42.3% for amorphous carbon. This suggests the presence of occluded solvents as well as some fraction of volatile impurity in the material. A scanning electron micrograph of thermally-treated carbonaceous material is shown in Fig. 3b. The separate CFs are visible in the image, the complete removal of all the amorphous content seems to be not possible by thermal treatment. A transmission electron micrograph of isolated fibers is presented in Fig. 4. The calculated fiber diameter falls in the range 200–300 nm and the length is few microns.

FTIR spectra of the as-prepared CFs and thermally-treated CFs are shown in Fig. 5a and b, respectively. The spectra reveal substantial amounts of Cl, H, N and O impurities in

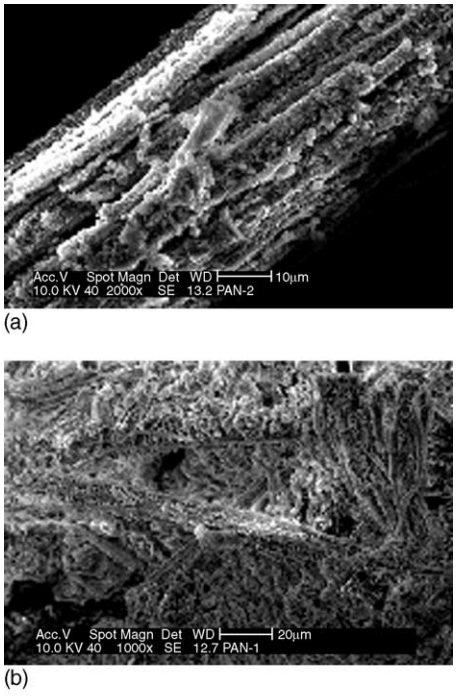

Fig. 3. Scanning electron micrograph in secondary electron imaging mode. (a) As-prepared carbon nanofibers; (b) after thermal treatment at 300 °C in air.

Fig. 4. Transmission electron micrograph of as-prepared nanofibers which shows isolated fibers of diameter 200–300 nm.

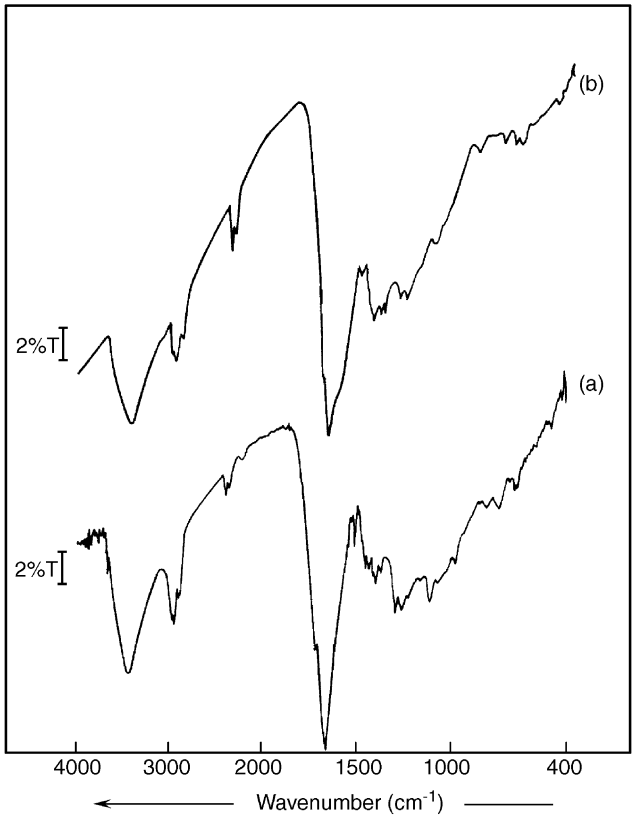

Fig. 5. FTIR spectra in range of 4400–450 cm^{-1}. Sample pellet prepared by mixing 1 mg of carbon material in 150 mg of KBr. (a) As-prepared carbon nanofibers; (b) after thermal treatment at 300 °C in air.

the form of functional moieties, such as –OH, =O, –COOH, etc. which are created during sample preparation. This is also consistent with the absence of characteristic C≡C stretching vibrations in IR spectra. Also, substituted carbon tetrachlorides are, in general, known to be reducible only to RC (R = H, methyl, phenyl) since C–H and C–C bonds are inert against reductive splitting. As higher capacitances can be achieved through surface conditioning of CFs, in particular, by anchoring a variety of surface functional groups using either thermal, chemical or electrochemical treatments [26], no attempt was made to obtain reduced CFs. Further, thermal treatment of CFs at 300 °C does not show a substantial change in the surface structure of CFs (Fig. 5b). The IR spectra of both as-prepared and thermally-treated CFs exhibit predominant absorption at ∼3427 and ∼1670 cm^{-1} which corresponds to –OH and C=O, respectively. The bands at ∼2922 and ∼2876 cm^{-1} can undoubtedly be assigned to aliphatic C–H stretches, and those at ∼1402 and ∼1376 cm^{-1} to C–H bending modes. The peaks at ∼1402 and ∼1376 cm^{-1} are likely to arise from encapsulated tetrabutylammonium ion [22]. The possible existence of C≡N species cannot be neglected in the present case, as the CFs are formed in acetonitrile solvent. The band at ∼2354 cm^{-1} indicates the presence of a C≡N moiety in the fibers. A –COOH impurity is also observed in the IR spectrum of the CFs, though it is not significant. The band at 1295 cm^{-1} represents C–O stretching, and C–O–H interaction appears at ∼1258 cm^{-1}. The band at ∼890 cm^{-1} can be assigned to the out-of-plane bending of bonded O–H. The appearance of the peak at ∼742 cm^{-1} corresponds to C–Cl stretching and is indicative of higher Cl content in electrochemically synthesized material. The observed peak shifts for functional groups are mainly due to the variety of their combinations.

The charge–discharge behavior at constant current in 6 M KOH electrolyte for as-prepared CFs is presented in Fig. 6. The system shows a significant sharp increase due to the ohmic drop at the beginning of the charging process as well

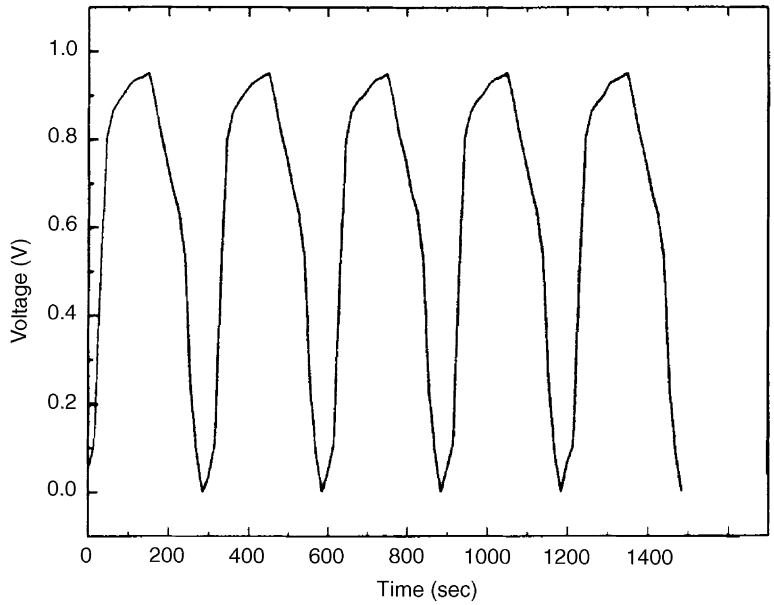

Fig. 6. Charge–discharge curve of CF electrode. Cell charged to 0.95 V at constant current of 0.6 mA and discharged at same current until voltage decrease to 0 V.

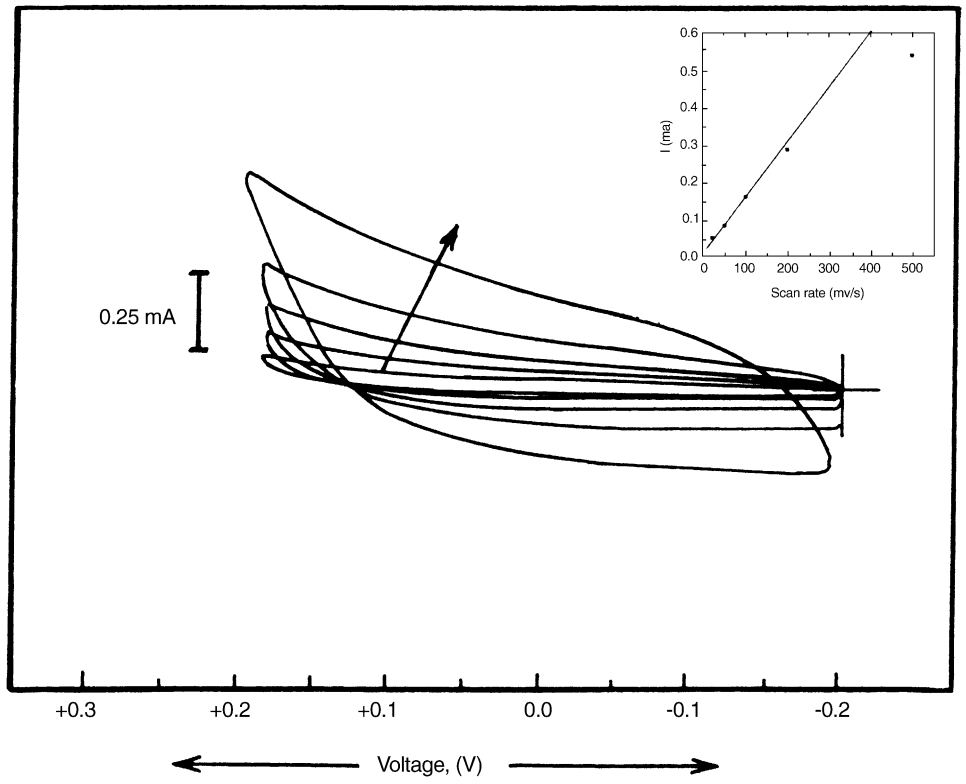

Fig. 7. Cyclic voltammogram for CF electrode recorded at various scan rates. Arrow indicates voltammogram at increasing scan rates (from 20 to 500 mV s^{-1}). Inset: plot of non-faradaic current vs. scan rate.

as during discharge. The BET surface-area of as-prepared carbon is 78 $m^2\ g^{-1}$, which allows an approximate estimation of 28 F g^{-1} for the specific capacitance from the discharge curve. Though the thermally-treated sample shows a remarkable increase in surface area, viz. 592 $m^2 g^{-1}$, the charge–discharge curve exhibits similar behavior and the capacitance value is practically constant. CFs generally exhibit a wide pore-size distribution which ranges from micropores (<20 Å) to macropores (>500 Å). On thermal annealing, due to pore opening some of the surface area can be accessed by ions. This increases the electrolytic resistance [14] because of the migration of ions in the pore and may be another factor which affects the overall capacitance of thermally-treated CFs. As the evaluated pore size of as-prepared CFs (23 Å) is nearly the same as that obtained for thermally-treated CFs (17 Å), the increased electrolytic resistance can lead to a fall in capacitance of the system. Moreover, as the prepared CFs in the present study also exhibit functionalized surfaces, hence, the results obtained apparently imply that thermal treatment may not improve the capacitive behavior of CFs electrochemically reduced from the chloroform precursor.

Additional insight to the capacitive behavior can be provided by cyclic voltammetric studies. Voltammograms recorded at room temperature for as-prepared CFs and taken in the range −0.2 to +0.2 V at various scan rates, are given in Fig. 7. The absence of faradaic peaks indicates capacitive charging and discharging at a constant rate over a complete cycle. An approximate estimation of capacitance is much lower than that obtained from charge–discharge measurements. The non-faradaic current is found, however, to vary linearly as a function of scan rate (as shown in the inset).

4. Conclusions

Electrochemically prepared carbon nanofibers reduced on a molybdenum electrode through a $CHCl_3$ precursor at room temperature exhibit capacitive behavior. The extracted CFs have a highly functionalized surface structure which includes species such as –OH, =O and –COOH. This carbonaceous material contains 24% CFs and shows a specific capacitance as high as 28 F g^{-1} estimated from the charge–discharge curves. A controlled rate of fibers formation as well as proper selection of the precursor may play key roles in determining the capacitive behavior of electrochemically synthesized carbon nanofibers.

Acknowledgements

Authors acknowledge Sophisticated Instrumentation Division, NCL for TEM facility. One of the authors PA thanks Dr. BK Das, Executive Director, C-MET, for granting permission to carry out this research. Authors SP and MT

thank CSIR India and DST India, respectively, for financial support.

References

[1] B.E. Conway, Electrochemical Supercapacitors—Scientific Fundamentals and Technological Applications, Kluwer Academic Publishers/Plenum Press, Dordrecht/New York, 1999.
[2] S.T. Mayer, R.W. Petala, J.L. Koschmitter, J. Electrochem. Soc. 140 (1993) 446.
[3] A. Yoshida, S. Nonaka, I. Aoki, A. Nishino, J. Power Sources 60 (1996) 213.
[4] E. Frackowaik, K. Méténier, T. Kyotani, S. Bonnamy, F. Béguin, Extended abstracts, in: Proceedings of the 24th Biennial Conference On Carbon, Vol. II, Charleston, SC, USA, American Carbon Society, 1999, pp. 544–545.
[5] E. Frackowaik, K. Méténier, R. Pelleng, S. Bonnamy, F. Béguin, Capacitance properties of carbon nanotubes, in: H. Kutzmany, et al. (Eds.), Electronic Properties of Novel Materials, 1999, pp. 429–432.
[6] S. Iijima, Nature 354 (1991) 56.
[7] T.W. Ebbesen, H.J. Lezec, H. Hiura, J.W. Bennette, H.F. Ghaemi, T. Thio, Nature 382 (1996) 54.
[8] J.P. Issi, L. Langer, J. Heremans, C.H. Olk, Carbon 33 (1995) 941.
[9] C. Nutzenadel, A. Zuttel, D. Chartouni, L. Schlaphach, Electrochem. Solid State Lett. 37 (1999) 61.
[10] C. Park, P.E. Anderson, A. Chambers, C.D. Tan, R. Hidalgo, N.M. Rodriguez, J. Phys. Chem. B 103 (1999) 10572.
[11] F. Leroux, K. Metenier, S. Gautier, E. Frackowiak, S. Bonnamy, F. Beguin, J. Power Sources 81-82 (1999) 317.
[12] G.T. Wu, C.S. Wang, X.B. Zhang, H.S. Yang, Z.F. Qi, P.M. He, W.Z. Li, J. Electrochem. Soc. 146 (1999) 1686.
[13] K.H. An, W.S. Kim, Y.S. Park, Y.C. Choi, S.M. Lee, D.C. Chung, D.J. Bae, S.C. Lim, Y.H. Lee, Adv. Mater. 13 (7) (2001) 497.
[14] C. Niu, E.K. Sichel, R. Hoch, D. Moy, H. Tennent, Appl. Phys. Lett. 70 (11) (1997) 1480.
[15] L. Diederich, E. Barborini, P. Piseri, A. Podesta, P. Milani, A. Scheneuwly, R. Gallay, Appl. Phys. Lett. 75 (17) (1999) 2662.
[16] Z. Cai, C.R. Martin, J. Am. Chem. Soc. 111 (1989) 4138.
[17] S. Serphin, D. Zhou, J. Jiao, M.A. Minke, S. Wang, T. Yadav, J.C. Withers, Chem. Phys. Lett. 217 (1994) 191.
[18] S. Iijima, T. Ichihashi, Nature 33 (1993) 603.
[19] R.T.K. Baker, Carbon 27 (1989) 315.
[20] P. Chitrapu, C.R.F. Lund, J.A. Tsamopoulos, Carbon 30 (1992) 285.
[21] L. Kavan, Chem. Rev. 97 (1997) 3061.
[22] R.D. Herrick II, A.S. Kaplan, B.K. Chinh, M.J. Shane, M.J. Sailor, K.L. Kavanagh, R.L. McCreery, J. Zhao, Adv. Mater. 7 (1995) 398.
[23] J.M. Moon, K.H. An, Y.H. Lee, Y.S. Park, D.J. Bae, G.S. Park, J. Phys. Chem. 97 (1993) 6941.
[24] H. Nishihara, H. Harada, S. Kaneko, M. Tateishi, K. Aramaki, J. Chem. Soc., Faraday Trans. 87 (8) (1991) 1187.
[25] X.Y. Zhu, S.M. Lee, Y.H. Lee, T. Frauenheim, Phys. Rev. Lett. 85 (2000) 2757.
[26] T. Momma, X. Liu, T. Osaka, Y. Ushio, Y. Sawada, J. Power Sources 60 (1996) 249.